

## Effect of partial sand replacement by coconut shell charcoal and silica fume in auto-claved aerated concrete an experimentation

Porcia Lawrence<sup>1</sup> , Jerlin Regin<sup>1</sup>

<sup>1</sup>St. Xavier's Catholic College of Engineering, Department of Civil Engineering, 629003, Kanyakumari, Tamil Nadu, India.

e-mail: lporcia@gmail.com, jerlin\_regin2003@yahoo.com

### ABSTRACT

Autoclaved Aerated Concrete (AAC) developed with Coconut Shell Charcoal (CSC) powder is a newly developed concrete with reasonable compressive strength and durability properties. The main idea of this study is to find out the applicability of CSC powder as partial replacement for fine aggregate in AAC, and the role of CSC in obtaining the strength and durability of AAC are discussed. In this study, material selection is done with reference to ASTM C1693-11 and CSC was used as a replacement material for river sand. CSC is an agricultural waste. Since the SiO<sub>2</sub> content of CSC is very low, Silica Fume (SF) is also used as fine aggregate replacement in addition to CSC to enhance the SiO<sub>2</sub> content. The specimens were made combining CSC and SF powders; CSC at 0%, 5%, 10%, 15% and 20% and SF at 0%, 1%, 2%, 3% and 4% by weight, and are coded as B0, B5, B10, B15 and B20 respectively. The developed AAC was analysed by conducting compressive strength, bulk density, thermal conductivity, scanning electron microscope (SEM) and X-ray diffraction (XRD) analyses. Additionally, water absorption, porosity, ultrasonic pulse velocity and acid attack tests were performed to determine the durability. XRD analysis showed the traces of C-S-H (Calcium Silicate Hydrate) gel and tobermorite peaks in B5 specimen, which produced enhanced compressive strength of 3.12 N/mm<sup>2</sup>. Thermal conductivity of the specimen with CSC replacement was between 0.218 to 0.186 W/m-K; it could be remarked from the results that the developed AAC is good in thermal insulation. Even though the porosity level reduced to 2% in B20 replacement, the specimens were light in weight, compared to B0. From the results obtained, it could be drawn the inference that CSC is a potential replacement for fine aggregate in AAC.

**Keywords:** Autoclaved aerated concrete; Coconut shell charcoal; Mechanical properties; Microstructure; Durability.

### 1. INTRODUCTION

AAC is being noticed due to its environmental friendly traits [1]. Generally, AAC is a porous, concrete which is light in weight as compared to conventional concrete [2]. The main constituents of AAC are cement, sand, water, gypsum, lime and aluminium powder. Aluminium powder, the aerating agent makes AAC a porous material, due to its chemical reaction with water, attributing AAC its mild weight and insulation qualities [3]. River sand is used as fine aggregate in the production of AAC. Unsustainable consumption of river sand destroys river beds, and in turn affects the ecological balance of rivers [4, 5]. Therefore, by considering the depletion of natural resources, a lot of studies have proved the usage of waste materials in place of the raw materials of AAC [6]. Agricultural wastes, industrial wastes and electronic wastes are used as fine and coarse aggregates replacement in conventional concrete [7–10]. Using these wastes in concrete can prevent environmental pollution and over utilization of river sand in construction.

KITTIPONG *et al.* [11] assessed the mechanical properties of AAC, by utilizing black rice husk and bagasse ashes in place of sand. Increase in compressive strength of AAC is witnessed with varied autoclaving temperatures and times. YUANMING *et al.* [12] conducted studies using municipal solid waste incineration bottom ash and found that the porosity property of incineration bottom ash of AAC improved while there was a decrease in the strength and stiffness with an increase in the amount of incineration bottom ash KURAMA *et al.* [13] made AAC with coal bottom ash and the results showed that the utilization of bottom ash in AAC formulations caused a decrease in the unit weight of the AAC for all replacement ratios of bottom ash. It was also found that for AAC with bottom ash contents of 25% and 50% had beneficial effects on strength gain. AGNIESZKA and WALDEMAR [14] utilized expanded perlite waste as a replacement for quartz sand and the

results showed that the expanded perlite waste is a silica source material for natural quartz that can be used in the manufacture of AAC. XIANGGUO *et al.* [15] studied the usage of municipal solid waste incineration bottom ash in AAC and observed that there was an increase in the compressive strength and the density of AAC when the fineness of municipal solid waste incineration bottom ash was increased. LAUKAITIS *et al.* [16] studied the utilization of fibrous additive in AAC; the findings showed that the fibrous additive could be an effective reinforcement. In latest studies bamboo cellulose, natural bamboo fiber and municipal solid waste were used to develop AAC and positive results were obtained [17–19]. The references mentioned above show that numerous wastes can be used to replace the raw materials in concrete production process.

India is the world's third largest producer of coconut [20]. Fifty billion coconuts are produced annually worldwide and 85% of coconut shells are thrown off as waste; these large portion of coconut shells are disposed in landfills. This land filling of coconut shells generates green house gases, especially methane and also creates soil and water pollution [21]. Another problem arises from the dumped waste that trigger fire risks in cultivated land [22] and also leads to breeding of mosquitoes and transmission of diseases [23]. This proves disposal of coconut shells to be a big problem in India [24]. And such problems can be solved by finding a right method for disposal of waste coconut shells [25]. Using the waste coconut shells in construction reduces waste management problem, leading to the protection and compensation of undersupply of natural fine aggregates [26, 27]. Developing concrete using coconut shell aggregates produced good compressive strength, bond strength, impact strength, tensile strength and flexural strength as that of conventional concrete [28]. Furthermore, coconut shell ash is a replacement for ordinary portland cement (OPC) due to its siliceous quality that can improve the strength. A number of studies have been carried out for determining the viability of utilizing coconut shell ash as an alternative material for cement replacement and positive results have been obtained [29].

No study has been carried out to explore the possible use of CSC as partial replacement of sand in AAC. The study presented here was to develop AAC including CSC as a partial replacement of sand to minimise the gap existing in past research. CSC has very low SiO<sub>2</sub> content [30]. Therefore, river sand is replaced with SF too, to replenish the SiO<sub>2</sub> content. In addition, SF has noticeable pozzolanic activity, larger specific surface area and reduced particle size that speed up the hydration process and generate more hydrated calcium silica gel that helps in enhanced strength properties of AAC. The SF also has filling effect which would improve the density of the porous structure, which in turn benefits in the enhancement of the mechanical properties of AAC [31]. This study is focused towards finding the effects of CSC and SF in the production of AAC. The obtained results would guide in using CSC as raw material in AAC.

## 2. MATERIALS AND METHODS

### 2.1. Materials

The materials employed for the production of AAC specimens are OPC (Grade 53), river sand, lime, gypsum, CSC, SF and aluminium powder aerating agent. Table 1 exhibits the chemical composition of the materials employed in this study. The river sand utilized in the study has an apparent density of 2.60 g/cm<sup>3</sup>. The XRD profiles of river sand and CSC are depicted in Figures 1 and 2. It was noted that the constituents of river sand

**Table 1:** Chemical composition of materials employed in this study.

| COMPOUNDS (%)                  | OPC   | RIVER SAND | CSC   | SF    | GYPSUM | LIME  |
|--------------------------------|-------|------------|-------|-------|--------|-------|
| SiO <sub>2</sub>               | 21.89 | 71.38      | 5.03  | 90.69 | 3.02   | 0.78  |
| Al <sub>2</sub> O <sub>3</sub> | 4.98  | 11.86      | 0.38  | 0.98  | 0.89   | 0.09  |
| CaO                            | 60.45 | 5.01       | 5.89  | 1.98  | 29.26  | 93.38 |
| MgO                            | 1.98  | 1.78       | 0.86  | 0.06  | 1.02   | 1.78  |
| Fe <sub>2</sub> O <sub>3</sub> | 4.01  | 2.95       | 0.56  | 0.45  | –      | 0.8   |
| K <sub>2</sub> O               | 0.34  | 1.56       | 44.96 | 0.15  | –      | 0.01  |
| SO <sub>3</sub>                | 3.02  | –          | 6.01  | 0.24  | 42.24  | –     |
| Na <sub>2</sub> O              | 0.40  | 1.30       | 16.03 | –     | –      | –     |
| LOI                            | 2.86  | 3.01       | –     | 3.6   | 21.36  | –     |
| P <sub>2</sub> O <sub>3</sub>  | –     | –          | 5.01  | –     | –      | –     |

LOI – Loss On Ignition.

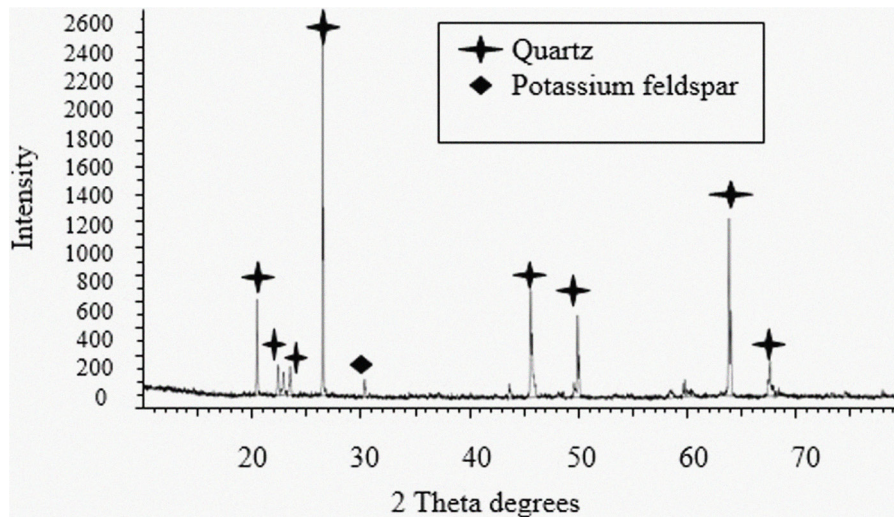


Figure 1: XRD profile of river sand.

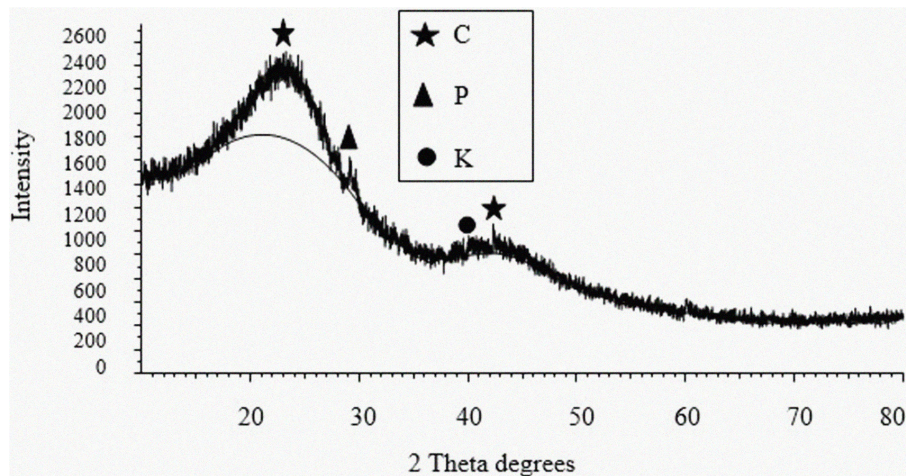


Figure 2: XRD profile of CSC.

are mainly quartz and potassium feldspar, and that of CSC is carbon (C), potassium (K) and phosphorus (P). Grading curve of river sand and CSC is exhibited in Figure 3. Grading classification curve is drawn by plotting particle size diameter along X-axis and cumulative passing percentage of particles along Y-axis. The sieving residue of river sand used was 8% above 100 $\mu\text{m}$  and that of CSC used was 2% above 40  $\mu\text{m}$ . River sand and CSC used in this study were well graded since particle size lies between 0.05 $\mu\text{m}$  to 120  $\mu\text{m}$  and 0.05  $\mu\text{m}$  to 50  $\mu\text{m}$  respectively. The particle diameters of D10 and D90 were found to be 32.49 and 92.48  $\mu\text{m}$  for river sand and 2.28 and 35.29  $\mu\text{m}$  for CSC respectively.

CSC is generally produced by burning coconut shells in limited supply of air enough for the carbonization of the coconut shells. The CSC used in this investigation was procured from a coconut charcoal producing industry in Tamil Nadu. The CSC used in the analysis had an apparent density of about 2.0 g/cm<sup>3</sup>. Table 2 shows the proportion of raw materials used in this study in weight percentage. Gypsum and lime are used to improve the performance of the concrete, gypsum is used to control the setting time of cement and adding suitable amount of lime improves the plasticity and workability.

## 2.2. Sample preparation

Preparing slurry is the first step in making AAC. Appropriate proportions of CSC, SF, river sand, lime, gypsum and OPC were thoroughly mixed with appropriate quantity of water to form slurry. In the slurry, aluminium powder and the aerating agent were added and blended well. A total of 70 cube specimens of



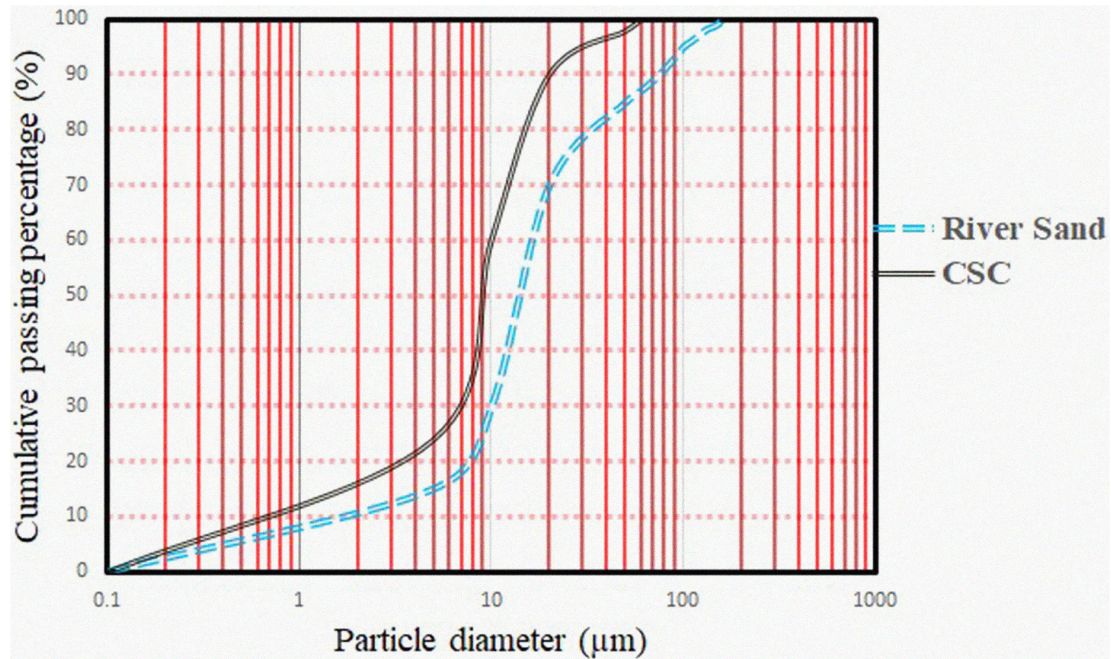


Figure 3: Grading curve of river sand and CSC.

Table 2: Proportion of raw materials used in this study in weight percentage.

| CONCRETE MIX | OPC | RIVER SAND | CSC | SF | LIME AND GYPSUM | AI   | AERATING AGENT |
|--------------|-----|------------|-----|----|-----------------|------|----------------|
| B0           | 9   | 68         | 0   | 0  | 23              | 0.13 | 0.02           |
| B5           | 9   | 62         | 5   | 1  | 23              | 0.13 | 0.02           |
| B10          | 9   | 56         | 10  | 2  | 23              | 0.13 | 0.02           |
| B15          | 9   | 50         | 15  | 3  | 23              | 0.13 | 0.02           |
| B20          | 9   | 44         | 20  | 4  | 23              | 0.13 | 0.02           |

Lime-Gypsum ratio 5:1, Water-Binder ratio 0.70.

size  $100 \times 100 \times 100$  mm were casted. 25 numbers for compressive strength test, 15 numbers for water absorption test, 15 numbers for porosity test and 15 numbers for acid attack test. To compute the thermal conductivity and bulk density, 15 cubes of size  $50 \times 50 \times 50$  mm and 15 prism specimens of size  $40 \times 40 \times 160$  mm, were developed. For pre-curing, the moulds were kept in an oven at  $60^\circ\text{C}$  to let gas formation by aluminium powder and the aerating agent. Finally, the demoulded specimens were autoclaved at  $120^\circ\text{C}$  and 2 MPa for 12 hours. Autoclaving is required for C-S-H and tobermorite formation [32]. Tobermorite formation is the most important effect of hydration of OPC and is formed during autoclaving. It is responsible for the strength of AAC. Figures 4 (a), (b), (c) and (d) exhibits the autoclaving machine, the developed samples, compression testing and ultrasonic pulse velocity tester.

### 2.3. Sample testing

The chemical compositions of materials were studied by X-ray fluorescence spectrometer and the distribution of particle size is analysed by laser particle size analyser. SEM with Energy dispersive X-ray (EDX) spectrometer was used to observe the micrographs of samples. Powder XRD patterns of river sand, CSC and developed samples were carried out with measuring range 10 to 70 degrees in  $2\theta$  with  $\text{CuK}_\alpha$  radiation. Compressive strength and bulk density were determined in accordance with ASTM C1693. To reduce the moisture content, the cured samples, used for compression testing were dried. Thermal conductivity test of AAC is done on  $50 \times 50 \times 50$  mm sized specimens in accordance with ASTM C177-13. ASTM C642-13 specification was used



**Figure 4:** Photos of (a) Autoclaving machine (b) Developed samples (c) Compression testing (d) Ultrasonic pulse velocity test.

to carryout water absorption test on the developed AAC specimens. Ultrasonic pulse velocity test was done using ultrasonic pulse velocity tester with transducer of 250 KHz. Porosity was calculated using

$$P = \left( 1 - \frac{m \times v^a}{m^a \times v} \right) \quad (1)$$

The volume ( $v$ ) and mass ( $m$ ) of the samples were measured. Then the samples were ground to powder, dried and its mass ( $m^a$ ) and volume ( $v^a$ ) were measured.

Acid attack test was primarily done to find the resistance of developed AAC to acid environment. The initial weight of the developed cubes was noted and immersed in 5% solution of sulfuric acid for 28 days, then removed and the compressive strength loss and weight loss were calculated.

### 3. RESULTS AND DISCUSSION

#### 3.1. Compressive strength and bulk density

Bulk density and compressive strength are important properties of AAC. Figures 5 (a) and (b) shows the compressive strengths and bulk densities of the prepared samples. There was a minor reduction in compressive strength and bulk density with the incorporation of CSC and SF when compared to B0. The mechanical properties of AAC are closely associated with the bulk density of the samples. The samples with decreased bulk density showed a decrease in the compressive strength too [33]. The samples with a reduction in bulk density from  $582 \text{ kg/m}^3$  to  $551 \text{ kg/m}^3$  showed a reduction in compressive strength from  $3.23 \text{ N/mm}^2$  to  $2.90 \text{ N/mm}^2$ . The decrease in compressive strength in turn decreases the development of tobermorite and C-S-H gel. The compressive strength is dependent on the pores of aerated mass, their shape, size, distribution [34], and tobermorite structure

formation. Lower compressive strength creates a crystalline phase of poor quality and prevents the formation of tobermorite. The B5 sample had the highest compressive strength of 3.12 N/mm<sup>2</sup> when CSC and SF were added. The compressive strength of B5 was roughly 0.11 N/mm<sup>2</sup> lower than B0 sample and 0.22 N/mm<sup>2</sup> higher than B20 sample. The developed AAC was a light weight material with lower compressive strength. Increased utilization of CSC powder may be the reason for reduction in compressive strength. The compressive strength of developed AAC is meeting the minimum strength requirement as specified in ASTM standard C1693-11, the values lie between the strength class of AAC-2 and AAC-4. The observation for the compressive strength test results is shown in Table 3.

### 3.2. XRD

The phase changes that occur during autoclaving are studied in XRD analysis. Phase composition of AAC depends upon the phase composition material used as cement replacement or raw material replacement. The composition of CSC is much intricate in contrast to the composition of coconut shell ash [31]. Figures 6 and 7 exhibit the XRD profiles of B5 and B20 specimens. In the XRD profile of B5 specimen, tobermorite and C-S-H gel formation were observed. Normally when silica sand is substituted with silica fume it improves the tobermorite formation [35]. C-S-H gel, in general, is an amorphous output brought about by the reaction of OPC or pozzolanic substances with water at room temperature [36]. As the percentage of CSC content was increased in B20 substitution, the tobermorite peak vanished. In B5 and B20 samples the traces of SiO<sub>2</sub> were missing. The loss of SiO<sub>2</sub> peaks is the consequence of the emergence of amorphous [37]. Tobermorite and C-S-H gel formation can be attributed to the reaction between CSC, SF, OPC, lime, gypsum and river sand.

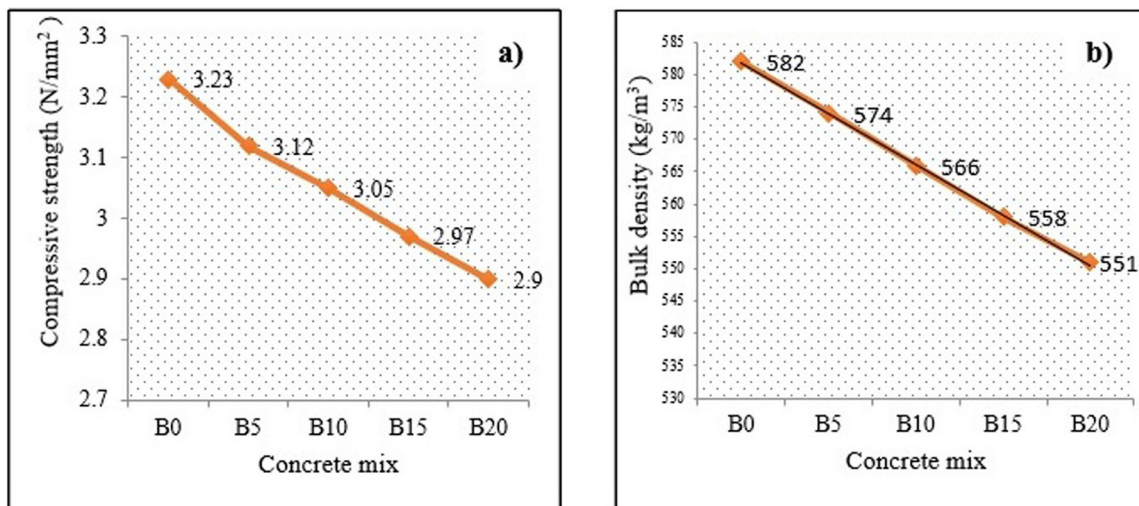


Figure 5: (a) Compressive strength and (b) Bulk densities of the developed AAC.

Table 3: Compressive strength of developed AAC with standard deviation.

| CONCRETE MIX | COMPRESSIVE STRENGTH (N/mm <sup>2</sup> ) (X) | AVERAGE STRENGTH (Y) | DEVIATION (X-Y) | STANDARD DEVIATION<br>$\sigma = \frac{\sqrt{\sum(X-Y)^2}}{\sqrt{N-1}}$ |
|--------------|---|----------------------|-----------------|--|
| B0           | 3.23  | 3.054                | 0.176           | 0  |
| B5           | 3.12  | 3.054                | 0.066           |  |
| B10          | 3.05  | 3.054                | -0.004          |  |
| B15          | 2.97  | 3.054                | -0.084          |  |
| B20          | 2.9   | 3.054                | -0.154          |  |



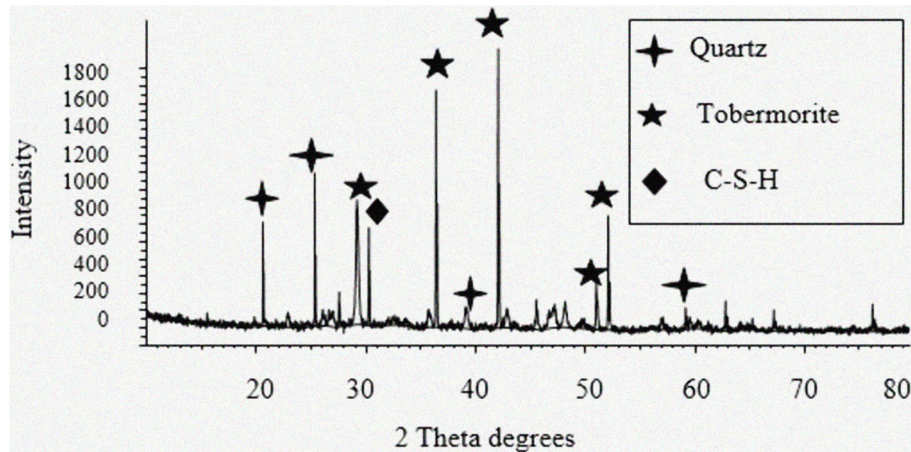


Figure 6: XRD profile of B5.

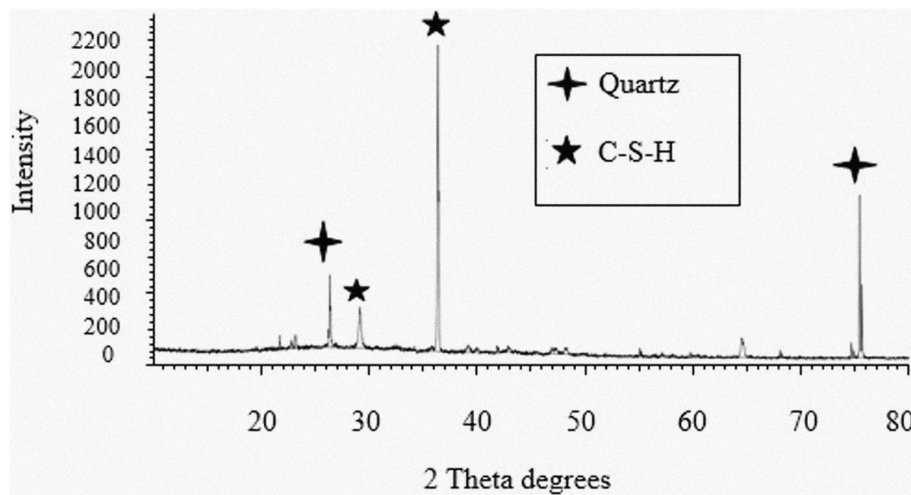


Figure 7: XRD profile of B20.

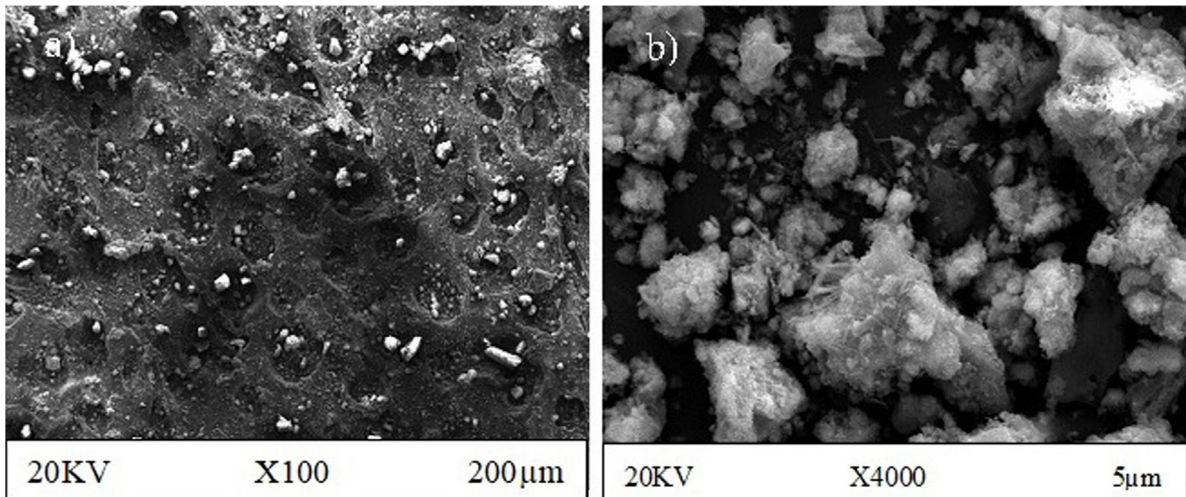
### 3.3. SEM

Figure 8 exhibits the SEM micrographs of the B5 sample. In the SEM images of B5 samples, at low magnification, pores formed could be observed; formation of pores is due to chemical reaction. At higher magnification, C-S-H gel formation was observed. C-S-H gel was formed as a result of hydration of AAC.

Figure 9 exhibits the SEM micrographs of the B20 sample. The type, amount and phase composition of the constituent materials influence the microstructure of AAC [38]. The micropores in the solid matrix and the macropores makes the AAC structure distinctive. Aeration brings macropores in AAC, as aeration tends to expand the concrete mass [39]. Addition of wastes changes the microstructure of the reaction product. It is evident from the Figure 8(a) of the samples that the pores formed in the AAC mass were independent and discontinuous forming an impermeable structure [40]. In Figure 8(b), large voids in abundance were observed; similar observations were found in [41]. A cluttered structure with small elements scattered could be seen in Figure 9(b); same structure was found in [42]. Weak crystalline C-S-H gel could be noticed in SEM micrographs of B5 and B20 samples at higher magnification. The C-S-H gel is responsible for the binding of the constituents of AAC forming a solid matrix to withstand the effects of loading [43, 44]. AAC microstructures rely on the type, phases existing in the matrix, rate of hydration, reaction product formed and how it is distributed in AAC matrix [45].

### 3.4. Thermal conductivity

Thermal conductivity is the property of a material to conduct heat. When compared to ordinary concrete the thermal conductivity of AAC will be lower [46]. The main functions of AAC are its strength and thermal



**Figure 8:** SEM images of B5 samples at (a) lower magnification and (b) higher magnification.

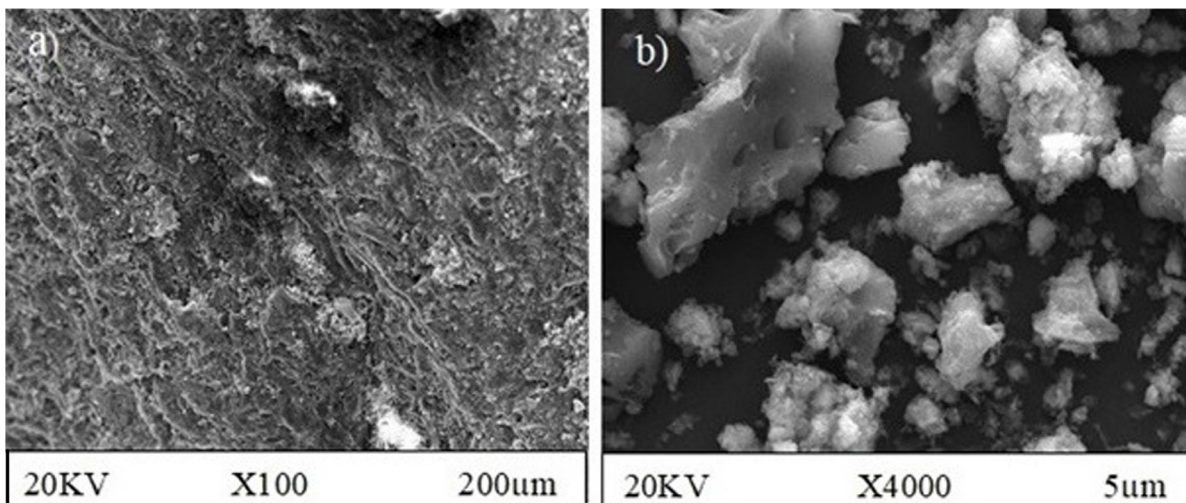


**Figure 9:** SEM images of B20 samples at (a) lower magnification and (b) higher magnification.

insulating property. The factors which affect the thermal conductivity are type of material, density and moisture content. Thermal conductivity results plotted in graph is shown in Figure 10(a). From the result, it could be understood that low bulk density was the reason for decrease in thermal conductivity. Materials with low thermal conductivity conduct very low heat, therefore from the result it is obvious that the developed AAC has good thermal insulation. The observations of bulk density, thermal conductivity, water absorption, ultrasonic pulse velocity and porosity tests are listed in Table 4.

### 3.5. Water absorption test

Water absorption of AAC increased with the replacement of river sand by CSC and SF. Usually CSC has higher water absorption rate when compared to that of river sand. Tobermorite formation densifies the microstructure which was the reason for decrease in water absorption in B0; similar observations were found in [47]. Water absorption capacity of AAC was large due to its porosity content and drainage passage. The CSC powder content increased the water absorption. The water absorption range was between 25.90% to 26.78% when the CSC powder concentration was between 0% and 20% by weight. Water absorption takes place by capillary pores and artificial air pores. Capillary pores volume doesn't vary but artificial air pores volume increases. The length for water movement also increases in the AAC material [48]. Bond strength is affected for the material which



**Table 4:** Bulk density, Thermal conductivity, Water absorption, Ultrasonic pulse velocity and Porosity of developed AAC with standard deviation.

| CONCRETE MIX | BULK DENSITY (kg/m <sup>3</sup> ) | THERMAL CONDUCTIVITY (W/m-K) | WATER ABSORPTION (%) | ULTRASONIC PULSE VELOCITY (km/sec) | POROSITY (%) | STANDARD DEVIATION<br>$\sigma = \frac{\sqrt{\sum(X-Y)^2}}{\sqrt{N-1}}$ |
|--------------|-----------------------------------|------------------------------|----------------------|------------------------------------|--------------|--|
| B0           | 582                               | 0.225                        | 25.9                 | 1.35                               | 73.9         | 0  |
| B5           | 574                               | 0.218                        | 26.02                | 1.46                               | 73.3         |  |
| B10          | 566                               | 0.208                        | 26.25                | 1.78                               | 72.6         |  |
| B15          | 558                               | 0.198                        | 26.52                | 2.01                               | 72.2         |  |
| B20          | 551                               | 0.186                        | 26.78                | 2.15                               | 71.9         |  |

has high water absorption. Water is absorbed from adhesive joints and this high value of absorption damages the walls and causes cracks in plasters [49]. Water absorption results plotted in graph is shown in Figure 10(b).

### 3.6. Ultrasonic pulse velocity test

The samples were tested by passing ultrasonic signal in the sample and calculating the time taken by the pulse to travel in the material. Slower velocities denote porosity and cracks in AAC samples and higher velocities denote decrease in porosity level. The ultrasonic pulse value of AAC samples will be 50% lower than that of conventional concrete. By the addition of CSC and SF the porosity of the developed AAC samples decreased, this was indicated by higher ultrasonic pulse velocity values among the developed specimens. The control mix specimen B0 had lower pulse velocity value. Ultrasonic pulse velocity results plotted in graph is shown in Figure 10(c).

### 3.7. Porosity

The porosity values plotted in graph is shown in Figure 10(d). Thermal insulation property of AAC is usually high, this is because of its high porosity level. The porosity values were not large as CSC content was increased. Higher porosity level is the reason for increase in moisture absorption; but in this case CSC may be the reason for increase in water absorption of AAC. Generally, there are two types of pores in AAC namely macropores and micropores. Pores having diameter more than 0.05  $\mu\text{m}$  are macropores and pores of size lesser than 0.002  $\mu\text{m}$  are micropores. Higher porosity level reduces the density of AAC [50]. Varying the foam content, increasing the stirring time are the methods for changing the size of pores and shaping the density. The porosity of B20 specimen decreased by 2% when compared to B0 specimen. The decrease in porosity was due to the addition of CSC, particle size, distribution of particles, shape of particles and fineness of the particles.

### 3.8. Acid attack test

Acid attack test results plotted in graph is shown in Figure 10(e). Since AAC is a porous material, the aggressive acid ions will easily penetrate in the concrete. The experimental results showed that, B0 was more resistant to acid attack resulting in lesser weight loss and strength loss, when compared to B20 specimen. In [51] it was reported that the reduction in compressive strength was due to the formation of gypsum and ettringite, which makes expansion and dissolution of cement paste in acid and make the cement matrix softer. Ettringite and gypsum formation were observed in [52].

## 4. CONCLUSION

This research utilizes CSC as a raw material in AAC as a substitution for river sand and the results concluded that CSC is a remarkable replacement for fine aggregate in AAC production. The developed B5 specimens showed the formation of tobermorite and C-S-H gel. This formation is because of the good bonding and reaction between the raw materials. In addition, this formation improves the compressive strength and acts as binding constituents in the solid matrix. However, the traces of tobermorite formation disappeared at 20% replacement. This disappearance of tobermorite peaks is the reason for the reduction in compressive strength and bulk density with increase in weight percent of CSC.

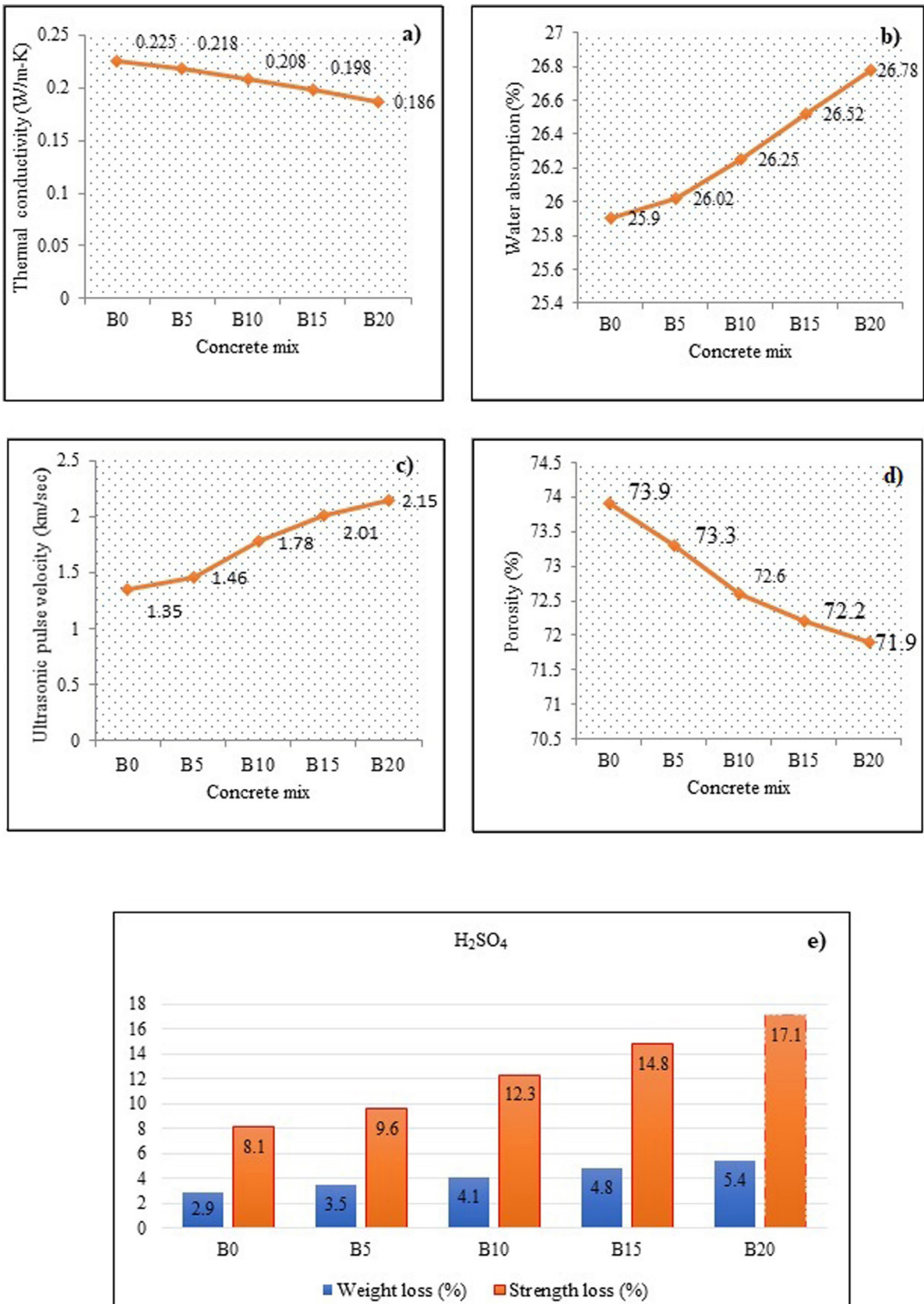


**Figure 10:** (a) Thermal conductivity (b) Water absorption (c) Ultrasonic pulse velocity (d) Porosity and (e) Acid attack test results of the developed AAC.

The compressive strengths of the developed specimens were in the range of 2.90 N/mm<sup>2</sup> to 3.23 N/mm<sup>2</sup>. The minimum compressive strength required for an AAC specimen according to ASTM C1693-11 for strength class AAC-2 is 2 MPa and for strength class AAC-4 is 4 MPa. Thus, CSC can be effectively utilized as a substitution for river sand to some extent which helps in preventing over utilization and exploitation of natural river sand.

Thermal insulation is an important requirement of AAC. The specimens with 20% CSC replacement showed better thermal insulation properties, when compared to B0 samples. The durability properties were evaluated by water absorption, porosity, ultrasonic pulse velocity and acid attack tests. Water absorption percent of AAC increased with the increase in weight percent of CSC. This is due to the higher water absorption ability of CSC. Even though the porosity level of the developed AAC with CSC replacement decreased, the developed specimen was light in weight with acceptable compressive strength. The decrease in porosity level is confirmed by higher ultrasonic pulse velocity. The durability of the developed AAC specimens against sulfuric acid attack was studied. Since AAC is a porous material, it is more prone to acid attack, as the acid ions will easily penetrate through the porous mass. The specimens without CSC content was more resistant to acid attack. The weight loss and strength loss percentages increased with increase in weight percent of CSC. The effect of SF was not observed in the XRD and SEM analysis, and this may be due to the very less replacement percentage of SF with fine aggregate. This coconut shell based charcoal waste is cheap and easy to produce, and its utilization in AAC proved to be a sustainable replacement for fine aggregate to some extent.

## 5. ACKNOWLEDGMENTS

The authors would like to thank St. Xavier's Catholic College of Engineering, Civil Engineering Department staff for assisting during research.

## 6. BIBLIOGRAPHY

- [1] XIAOLING, Q., XUGUANG, Z., "Previous and present investigations on the components, microstructure and main properties of autoclaved aerated concrete: a review", *Construction & Building Materials*, v. 135, pp. 505–516, 2017. doi: <http://doi.org/10.1016/j.conbuildmat.2016.12.208>.
- [2] HUIWEN, W., YONG, H., GANG, L., *et al.*, "Study on the structure and properties of autoclaved aerated concrete produced with the stone-sawing mud", *Construction & Building Materials*, v. 184, pp. 20–26, 2018. doi: <http://doi.org/10.1016/j.conbuildmat.2018.06.214>.
- [3] JUN, J., QIANG, C., BING, M., *et al.*, "Effect of ZSM-5 waste dosage on the properties of autoclaved aerated concrete", *Construction & Building Materials*, v. 278, pp. 122114, 2021. doi: <http://doi.org/10.1016/j.conbuildmat.2020.122114>.
- [4] RENTIER, E.S., CAMMERAAT, L.H., "The environmental impacts of river sand mining", *The Science of the Total Environment*, v. 838, n. Pt 1, pp. 155877, 2022. doi: <http://doi.org/10.1016/j.scitotenv.2022.155877>. PubMed PMID: 35569654.
- [5] DINH, H.L., LIU, J., DOMINIC, E.L., *et al.*, "A sustainable solution to excessive river sand mining by utilizing by-products in concrete manufacturing: a state of the art review", *Cleaner Materials*, v. 6, pp. 100140, 2022. doi: <http://doi.org/10.1016/j.clema.2022.100140>.
- [6] QIANG, C., BING, M., JUN, J., *et al.*, "Utilization of waste red gypsum in autoclaved aerated concrete preparation", *Construction & Building Materials*, v. 291, pp. 123376, 2021. doi: <http://doi.org/10.1016/j.conbuildmat.2021.123376>.
- [7] AGUIAR, J.G.C., SOUZA, M.M.D., FARIAS, E.C.D., "Development of lightweight aggregates from coffee grounds and rice husk ash", *Matéria (Rio de Janeiro)*, v. 29, n. 1, pp. e20230313, 2024. doi: <http://doi.org/10.1590/1517-7076-rmat-2023-0313>.
- [8] RAJESH, A.A., SENTHILKUMAR, S., SARGUNAN, K., *et al.*, "Interpolation and extrapolation of flexural strength of rubber crumbs and coal ash with graphene oxide concrete", *Matéria (Rio de Janeiro)*, v. 28, n. 4, pp. e20230179, 2023. doi: <http://doi.org/10.1590/1517-7076-rmat-2023-0179>.
- [9] MELLO, P.H.C., ALTOÉ, S.P.S., GDIRÃO, G.S.D.M., *et al.*, "Mechanical analysis of concrete with partial replacements of aggregates by steel filings", *Matéria (Rio de Janeiro)*, v. 29, pp. e20230325, 2024. doi: <http://doi.org/10.1590/1517-7076-rmat-2023-0325>.
- [10] RAMASAMY, S., SOUNDARARAJAN, E.K., VISWANATHAN, R., *et al.*, "An analysis of the durability features and strength of the E-waste concrete", *Matéria (Rio de Janeiro)*, v. 29, n. 2, pp. e20240108, 2024. doi: <http://doi.org/10.1590/1517-7076-rmat-2024-0108>.



- [11] KITTIPONG, K., SUWIMOL, A., SUTHATIP, S., “Influence of partial sand replacement by black rice husk ash and bagasse ash on properties of autoclaved aerated concrete under different temperatures and times”, *Construction & Building Materials*, v. 173, pp. 220–227, 2018. doi: <http://doi.org/10.1016/j.conbuildmat.2018.04.043>.
- [12] YUANMING, S., BAOLING, L., EN-HUA, Y., *et al.*, “Feasibility study on utilization of municipal solid waste incineration bottom ash as aerating agent for the production of autoclaved aerated concrete”, *Cement and Concrete Composites*, v. 56, pp. 51–58, 2015. doi: <http://doi.org/10.1016/j.cemconcomp.2014.11.006>.
- [13] KURAMA, H., TOPCU, I.B., KARAKURTH, C., “Properties of the autoclaved aerated concrete produced from coal bottom ash”, *Journal of Materials Processing Technology*, v. 209, n. 2, pp. 767–773, 2009. doi: <http://doi.org/10.1016/j.jmatprotec.2008.02.044>.
- [14] AGNIESZKA, R., WALDEMAR, P., “Effect of perlite waste addition on the properties of autoclaved aerated concrete”, *Construction & Building Materials*, v. 120, pp. 65–71, 2016. doi: <http://doi.org/10.1016/j.conbuildmat.2016.05.019>.
- [15] XIANGGUO, L., ZHUOLIN, L., YANG, L., *et al.*, “Utilization of municipal solid waste incineration bottom ash in autoclaved aerated concrete”, *Construction & Building Materials*, v. 178, pp. 175–182, 2018. doi: <http://doi.org/10.1016/j.conbuildmat.2018.05.147>.
- [16] LAUKAITIS, A., KERIENE, J., MIKULSKIS, D., *et al.*, “Influence of fibrous additives on properties of aerated autoclaved concrete forming mixtures and strength characteristics of products”, *Construction & Building Materials*, v. 23, n. 9, pp. 3034–3042, 2009. doi: <http://doi.org/10.1016/j.conbuildmat.2009.04.007>.
- [17] JIE, Z., FEI, H., YUCHAO, W., *et al.*, “Mechanical properties and interface improvement of bamboo cellulose nanofibers reinforced autoclaved aerated concrete”, *Cement and Concrete Composites*, v. 134, pp. 104760, 2022. doi: <http://doi.org/10.1016/j.cemconcomp.2022.104760>.
- [18] WENLI, Q., WEI, H., YONGJIANNAN, A., *et al.*, “The effect of natural bamboo fiber and basalt fiber on the properties of autoclaved aerated concrete”, *Construction & Building Materials*, v. 377, pp. 131153, 2023. doi: <http://doi.org/10.1016/j.conbuildmat.2023.131153>.
- [19] YIQUAN, L., DHANENDRA, K., KANG, H.L., *et al.*, “Efficient utilization of municipal solid wastes incinerator bottom ash for autoclaved aerated concrete formulation”, *Journal of Building Engineering*, v. 71, pp. 106463, 2023. doi: <http://doi.org/10.1016/j.jobe.2023.106463>.
- [20] KUKKEHALLI, B.H., PULLOOTT, S.A., VELIYATHUKUDY, S.J., “Predicting the potential suitable climate for coconut (*cocos nucifera* L.) cultivation in India under climate change scenarios using the maxent model”, *Plants*, v. 11, n. 6, pp. 731, 2022. doi: <http://doi.org/10.3390/plants11060731>. PubMed PMID: 35336613.
- [21] KAVISHAN, S.R., ENRIQUE, R.C., CHARLOTTE, L.T., “Evaluation of the optimal concrete mix design with coconut shell ash as a partial cement replacement”, *Construction & Building Materials*, v. 401, pp. 132978, 2023. doi: <http://doi.org/10.1016/j.conbuildmat.2023.132978>.
- [22] HAIBAO, L., QIUYI, L., PEIHAN, W., “Assessment of the engineering properties and economic advantage of recycled aggregate concrete developed from waste clay bricks and coconut shells”, *Journal of Building Engineering*, v. 68, pp. 106071, 2023. doi: <http://doi.org/10.1016/j.jobe.2023.106071>.
- [23] LUANE, A.N., MARIA, L.S., JULIANO, G., *et al.*, “Waste green coconut shells Diagnosis of the disposal and applications for use in other products”, *Journal of Cleaner Production*, v. 255, pp. 120169, 2020. doi: <http://doi.org/10.1016/j.jclepro.2020.120169>.
- [24] RADHA, T., KAMAL, K., HEMANTH, S.P., *et al.*, “A comprehensive study of waste coconut shell aggregate as raw material in concrete”, *Materials Today: Proceedings*, v. 44, pp. 437–443, 2021. doi: <http://doi.org/10.1016/j.matpr.2020.09.754>.
- [25] SUJATHA, S., DEEPA, B., “Properties of high strength lightweight concrete incorporating crushed coconut shells as coarse aggregate”, *Materials Today: Proceedings*, 2023. In press. doi: <http://doi.org/10.1016/j.matpr.2023.03.201>.
- [26] SUJATHA, A., DEEPA, B., “Development of high strength lightweight coconut shell aggregate concrete”, *Current Trends in Civil Engineering*, v. 104, pp. 95–103, 2021. doi: [http://doi.org/10.1007/978-981-15-8151-9\\_10](http://doi.org/10.1007/978-981-15-8151-9_10).
- [27] SIDDHARTHA, B., MANOJ, A., BHASKAR, S., “Usage potential and benefits of processed coconut shells in concrete as coarse aggregates”, *Materials Today: Proceedings*, 2023. In press. doi: <http://doi.org/10.1016/j.matpr.2023.03.529>.

- [28] BARI, H., SALAM, M.A., SAFIUDDIN, M., “Fresh and hardened properties of brick aggregate concrete including coconut shell as a partial replacement of coarse aggregate”, *Construction & Building Materials*, v. 297, pp. 123745, 2021. doi: <http://doi.org/10.1016/j.conbuildmat.2021.123745>.
- [29] NARAINDAS, B., SANTOSH, K.M., ADEYEMI, A., “Influence of coconut shell ash on workability, mechanical properties, and embodied carbon of concrete”, *Environmental Science and Pollution Research International*, v. 28, n. 5, pp. 5682–5692, 2021. doi: <http://doi.org/10.1007/s11356-020-10882-1>. PubMed PMID: 32970258.
- [30] ANDRIANI, R., DWIKI, P., “Utilization of coconut shell charcoal to improve bearing capacity of clay as subgrade for road pavement”, *IOP Conference Series. Earth and Environmental Science*, v. 832, n. 1, pp. 012041, 2021. doi: <http://doi.org/10.1088/1755-1315/832/1/012041>.
- [31] WUDI, F., ZHEN, L., QING, L., “Study on the properties of autoclaved aerated concrete with high content concrete slurry waste”, *Developments in the built environment*, v. 17, pp. 100338, 2024. doi: <http://doi.org/10.1016/j.dibe.2024.100338>.
- [32] TABAN, S., GEORG, S., DETLEF, H., *et al.*, “Production of autoclaved aerated concrete with silica raw materials of a higher solubility than quartz part II: Influence of autoclaving temperature”, *Construction & Building Materials*, v. 287, pp. 123072, 2021. doi: <http://doi.org/10.1016/j.conbuildmat.2021.123072>.
- [33] RONGSHENG, X., TINGSHU, H., YONGQI, D., “Utilizing Wood fiber produced with wood waste to reinforce autoclaved aerated concrete”, *Construction & Building Materials*, v. 208, pp. 242–249, 2019. doi: <http://doi.org/10.1016/j.conbuildmat.2019.03.030>.
- [34] YUAN, B., STRAUB, C., SEGERS, S., *et al.*, “Sodium carbonate activated slag as cement replacement in autoclaved aerated concrete”, *Ceramics International*, v. 43, n. 8, pp. 6039–6047, 2017. doi: <http://doi.org/10.1016/j.ceramint.2017.01.144>.
- [35] HAMDY, E., “Fabrication and properties of autoclaved aerated concrete containing agriculture and industrial solid wastes”, *Journal of Building Engineering*, v. 22, pp. 528–538, 2019. doi: <http://doi.org/10.1016/j.jobbe.2019.01.023>.
- [36] JUN, J., BING, M., QIANG, C., *et al.*, “Utilization of ZSM-5 waste for the preparation of autoclaved aerated concrete (AAC): Mechanical properties and reaction products”, *Construction & Building Materials*, v. 297, pp. 123821, 2021. doi: <http://doi.org/10.1016/j.conbuildmat.2021.123821>.
- [37] Zhitao, C., Yiquan, L., Weiping, Z., *et al.*, “Incinerator bottom ash (IBA) aerated geopolymer”, *Construction & Building Materials*, v. 112, pp. 1025–1031, 2016. doi: <http://doi.org/10.1016/j.conbuildmat.2016.02.164>.
- [38] TINGSHU, H., RONGSHENG, X., YONGQI, D., *et al.*, “Experimental study of high- performance autoclaved aerated concrete produced with recycled wood fibre and rubber powder”, *Journal of Cleaner Production*, v. 234, pp. 559–567, 2019. doi: <http://doi.org/10.1016/j.jclepro.2019.06.276>.
- [39] CENK, K., HALDUN, K., ILKER, B.T., “Utilization of natural zeolite in aerated concrete production”, *Cement and Concrete Composites*, v. 32, n. 1, pp. 1–8, 2010. doi: <http://doi.org/10.1016/j.cemconcomp.2009.10.002>.
- [40] ZUHTU, O.P., IBRAHIM, U., ZEYNEP, P., *et al.*, “The effect of different fiber reinforcement on the thermal and mechanical properties of autoclaved aerated concrete”, *Construction & Building Materials*, v. 112, pp. 325–330, 2016. doi: <http://doi.org/10.1016/j.conbuildmat.2016.02.223>.
- [41] FAZEL, S., GHASEM, P., SEYYEDEH, B.S., “A study of mechanical and microstructures properties of autoclaved aerated concrete containing nano-graphene”, *Journal of Building Engineering*, v. 43, pp. 103106, 2021. doi: <http://doi.org/10.1016/j.jobbe.2021.103106>.
- [42] RENDI, W., SHAOBIN, D., SHOUWEI, J., *et al.*, “Utilization of solid waste high-volume calcium coal gangue in autoclaved aerated concrete: Physico-mechanical properties, hydration products and economic costs”, *Journal of Cleaner Production*, v. 278, pp. 123416, 2021. doi: <http://doi.org/10.1016/j.jclepro.2020.123416>.
- [43] WANG, C., WEN, N., SI-QI, Z., *et al.*, “Preparation and properties of autoclaved aerated concrete using coal gangue and iron ore tailings”, *Construction & Building Materials*, v. 104, pp. 109–115, 2016. doi: <http://doi.org/10.1016/j.conbuildmat.2015.12.041>.
- [44] KEUN-HYEOK, Y., KYUNG-HO, L., “Tests on high-performance aerated concrete with a lower density”, *Construction & Building Materials*, v. 74, pp. 109–117, 2015. doi: <http://doi.org/10.1016/j.conbuildmat.2014.10.030>.

- [45] AGNIESZKA, R., LUKASZ, K., “Waste originating from the cleaning of flue gases from the combustion of industrial wastes as a lime partial replacement in autoclaved aerated concrete”, *Materials (Basel)*, v. 15, n. 7, pp. 2576, 2022. doi: <http://doi.org/10.3390/ma15072576>. PubMed PMID: 35407906.
- [46] IMAN, A., PAYAM, S., ZAHIRUDDIN, F.B.A.H., *et al.*, “Thermal conductivity of concrete- A review”, *Journal of Building Engineering*, v. 20, pp. 81–93, 2018. doi: <http://doi.org/10.1016/j.job.2018.07.002>.
- [47] SARBJEET, S., RAVINDRA, N., VINAY, A., *et al.*, “Sustainable utilization of granite cutting waste in high strength concrete”, *Journal of Cleaner Production*, v. 10, pp. 223–235, 2016. doi: <http://doi.org/10.1016/j.jclepro.2015.12.110>.
- [48] ABDUL, R.R., AHMAD, F., ATTHAKORN, T., “The physical and mechanical properties of autoclaved aerated concrete with recycled AAC as a partial replacement for sand”, *Buildings*, v. 12, n. 1, pp. 60, 2022. doi: <http://doi.org/10.3390/buildings12010060>.
- [49] AVADHOOT, B., NIKHIL, P.Z., ROBIN, D., *et al.*, “Experimental investigation of autoclaved aerated concrete masonry”, *Journal of Materials in Civil Engineering*, v. 7, n. 7, pp. 31, 2019. doi: [http://doi.org/10.1061/\(ASCE\)MT.1943-5533.0002762](http://doi.org/10.1061/(ASCE)MT.1943-5533.0002762).
- [50] GUGLIELMI, P.O., SILVA, W.R.L., REPETTE, W.L., *et al.*, “Porosity and mechanical strength of an autoclaved clayey cellular concrete”, *Advances in Civil Engineering*, v. 6, pp. 1–6, 2010. doi: <http://doi.org/10.1155/2010/194102>.
- [51] JAVAD, D., MAHDI, N., “Compressive and direct tensile behavior of concrete containing Forta- Ferro fiber and calcium aluminate cement subjected to sulfuric acid attack with optimized design”, *Construction & Building Materials*, v. 253, pp. 118999, 2020. doi: <http://doi.org/10.1016/j.conbuildmat.2020.118999>.
- [52] MAHDI, S., HESAM, K., MOSTAFA, H., *et al.*, “Sulfuric acid resistance of concrete containing coal waste as a partial substitute for fine and coarse aggregates”, *Fuel*, v. 348, pp. 128311, 2023. doi: <http://doi.org/10.1016/j.fuel.2023.128311>.